Published in final edited form as:
Bone. 2012 January ; 50(1): 209–217. doi:10.1016/j.bone.2011.10.025.

Sost downregulation and local Wnt signaling are required for the osteogenic response to mechanical loading

Xiaolin Tu[1], **Yumie Rhee**[1,5], **Keith Condon**[1], **Nicoletta Bivi**[1], **Matthew R. Allen**[1], **Denise Dwyer**[4], **Marina Stolina**[4], **Charles H. Turner**[3], **Alexander G. Robling**[1], **Lilian I. Plotkin**[1], and **Teresita Bellido**[*,1,2]

Xiaolin Tu: xtu@iupui.edu; Yumie Rhee: yumie@yuhs.ac; Keith Condon: kcondon@iupui.edu; Nicoletta Bivi: nicobivi@iupui.edu; Matthew R. Allen: matallen@iupui.edu; Denise Dwyer: ddwyer@amgen.com; Marina Stolina: mstolina@amgen.com; Alexander G. Robling: arobling@iupui.edu; Lilian I. Plotkin: lplotkin@iupui.edu

[1]Department of Anatomy and Cell Biology, Indiana University School of Medicine, Indianapolis, IN, USA

[2]Department of Medicine, Division of Endocrinology, Indiana University School of Medicine, Indianapolis, IN, USA

[3]Department of Orthopedic Surgery, Biomechanics and Biomaterials Research Center, Indiana University School of Medicine, Indianapolis, IN, USA

[4]Metabolic Research Department, Amgen Inc., Thousand Oaks, CA, USA

Abstract

Sclerostin, the Wnt signaling antagonist encoded by the *Sost* gene, is secreted by osteocytes and inhibits bone formation by osteoblasts. Mechanical stimulation reduces sclerostin expression, suggesting that osteocytes might coordinate the osteogenic response to mechanical force by locally unleashing Wnt signaling. To investigate whether sclerostin downregulation is a pre-requisite for load-induced bone formation, we conducted experiments in transgenic mice (TG) engineered to maintain high levels of *SOST* expression during mechanical loading. This was accomplished by introducing a human *SOST* transgene driven by the 8kb fragment of the DMP1 promoter that also provided osteocyte specificity of the transgene. Right ulnae were subjected to *in vivo* cyclic axial loading at equivalent strains for 1 min/day at 2Hz; left ulnae served as internal controls. Endogenous murine *Sost* mRNA expression measured 24h after 1 loading bout was decreased by about 50% in TG and wild type (WT) littermates. In contrast, human *SOST*, only expressed in TG mice, remained high after loading. Mice were loaded on 3 consecutive days and bone formation was quantified 16 days after initiation of loading. Periosteal bone formation in control ulnae was similar in WT and TG mice. Loading induced the expected strain-dependent increase in bone formation in WT mice, resulting from increases in both mineralizing surface (MS/BS) and mineral apposition rate (MAR). In contrast, load-induced bone formation was reduced by 70–85% in TG mice, due to lower MS/BS and complete inhibition of MAR. Moreover, Wnt target gene expression induced by loading in WT mice was absent in TG mice. Thus, downregulation of *Sost*/

[*]Corresponding author and reprint requests: Teresita Bellido, Ph.D., Department of Anatomy and Cell Biology, and Department of Internal Medicine, Division of Endocrinology, Indiana University School of Medicine, 635 Barnhill Drive, MS5035, Indianapolis, IN 46202, Phone 317-274-7410, Fax 317-278-2040, tbellido@iupui.edu.
[5]Current address: Department of Internal Medicine, College of Medicine, Yonsei University, Seoul, Korea

Conflict of interest: The authors declare that no conflict of interest exists.

sclerostin in osteocytes is an obligatory step in the mechanotransduction cascade that activates Wnt signaling and directs osteogenesis to where bone is structurally needed.

Keywords

Osteocytes; *Sost*; sclerostin; mechanical loading; bone formation; Wnt signaling

Introduction

The skeleton adapts to meet mechanical needs by changing its mass, shape, and microarchitecture [1–3]. Osteocytes (former osteoblasts buried in the bone matrix) are proposed to act as mechanosensors [4]. Whereas bone-forming osteoblasts and bone-resorbing osteoclasts are present on bone surfaces for relatively short periods of time and in low numbers, osteocytes are by far the most abundant resident cells and are present throughout the entire bone tissue. Osteocytes are also the core of a functional syncytium that extends from the mineralized bone matrix to the bone surface and the bone marrow, reaching the blood vessels. Their abundance and strategic location make osteocytes the most suitable candidates for detecting variations in the level of strain and for distributing signals leading to adaptive responses [5].

Regulation of the expression of sclerostin, a glycoprotein encoded by the *Sost* gene, has emerged as a compelling mechanism by which osteocytes control the activity of bone remodeling cells [6]. This protein is secreted by osteocytes and acts in a paracrine (and potentially autocrine) fashion to inhibit bone formation by antagonizing the pro-differentiating and survival actions of Wnts in osteoblasts. Genetic and pharmacologic evidence supports this mechanism. Loss of *SOST* expression in humans causes the high bone mass disorders Van Buchem's disease [7] and sclerosteosis [8]. Mice with targeted deletion of the *Sost* gene also display progressive high bone mass and increased bone strength [9, 10]; whereas, conversely, transgenic mice overexpressing *SOST* exhibit low bone mass [11–13]. Pharmacologic inhibition of sclerostin with neutralizing antibodies leads to marked anabolic effects in several preclinical osteopenic animal models and has been met with promising results in clinical settings [6, 14]. Sclerostin is also regulated by hormonal stimuli that affect the skeleton. In particular, elevation of parathyroid hormone (PTH), either in an intermittent or a continuous mode, downregulates sclerostin expression in osteocytes in mice and decreases the circulating levels of the protein in humans [15–19].

Mechanical forces are essential for the development, growth, and maintenance of the skeleton. Skeletal sites subjected to high mechanical strains exhibit high bone formation, whereas unloaded bones display reduced bone formation. These adaptive responses of the skeleton are thought to be mediated by osteocytes and to result from regulation of the Wnt signaling pathway [4]. Using the murine ulnar loading model [20], we have demonstrated that cortical bone areas exposed to high mechanical strain exhibit a reduction in sclerostin-positive osteocytes that is associated with higher bone formation on adjacent periosteal surfaces [21]. This evidence suggested that osteocytes coordinate the osteogenic response to mechanical force by downregulating sclerostin, thereby locally unleashing Wnt signaling. We now show that mice overexpressing a human *SOST* transgene in osteocytes, which is not downregulated by loading, failed to exhibit activation of the Wnt pathway and the anabolic response to mechanical stimulation. Thus, *Sost* downregulation is an obligatory step for mechanotransduction.

Materials and Methods

DMP1-*SOST* transgenic mice

DMP1-*SOST* transgenic mice were generated by inserting the human *SOST* cDNA (I.M.A.G.E. clone ID: 40009482, American Tissue Culture Collection, Manassas, VA) downstream from a DNA fragment containing 8 kb of the 5′-flanking region, the first exon, the first intron, and 17 bp of exon 2 of the murine dentin matrix protein 1 (DMP1) gene [22], and upstream from a 140 bp fragment containing the rabbit beta-globin polyadenylation sequence, as previously described [13]. Hemizygous DMP1-*SOST* mice or wild type littermates were used in the experiments. Mice were fed a regular diet (Harlan/Teklad #7001, Indianapolis, IN) and water ad libitum and maintained on a 12-h light/dark cycle. Protocols were approved by the Institutional Animal Care and Use Committee of Indiana University School of Medicine.

Bone mineral density (BMD) measurement and micro-computed tomography (Micro-CT) analysis

Four, 8, and 16 week-old mice were anesthetized via inhalation of 2.5% isoflurane (Abbott Laboratories, Abbott Park, IL) mixed with O_2 (1.5 liter/min) and BMD of the total body, excluding the head and the tail, lumbar spine (L1-6), and femur was measured by dual energy x-ray absorptiometry (DXA) using a PIXImus II densitometer (G.E. Medical Systems, Madison, WI), as previously described [23]. For micro-CT analysis, bones from 6, 10, and 16 week-old mice were dissected, cleaned off soft tissue, fixed in 10% buffered formalin, and stored in 70% ethanol until scanned at 6 micron resolution (Skyscan 1172, SkyScan, Kontich, Belgium). Bone length was measured using a digital sliding caliper after removing the soft tissue.

Ulna strain measurements

Strain levels at the midshaft ulna were measured in a cohort of 6 female mice at 16 weeks of age to derive the relation between applied force and mechanical strain for both genotypes, as previously published [24]. Briefly, the right forearm was dissected to expose the lateral surface of the ulnar diaphysis, and a miniature (EA-015DJ-120; Vishay, Inc.) single element strain gauge was bonded to the midshaft. The forearm was then placed in a computer-controlled electromagnetic mechanical actuator (Bose, Eden Prairie, MN), and exposed to cyclic axial compression using a 2-Hz haversine waveform. The peak force was progressively increased with each cycle, and ranged from 1.2 to 2.4 N. During loading, conditioned voltage output from the strain gauge and output from the load cell were recorded and processed as previously described [20]. Voltage output was converted to strain using previously described calibration procedures. From these data the force:strain relation was derived for both genotypes individually, and low, medium, and high loads for in vivo mechanical loading were calculated so that 2460, 2850, and 3240 με were generated, respectively, in both genotypes.

In vivo ulnar loading

To examine the effect of loading on bone formation, mice were loaded 1 min per day during 3 consecutive days and bones were collected after 16 days of initiation of loading to perform dynamic histomorphometry. Previous extensive evidence had shown that this loading regimen and timing of measurement is the optimal to detect the increased bone formation in areas of cortical bone exposed to high mechanical strain [20, 24]. Six to 8 female mice per group at 16 weeks of age were loaded on the right forearm for 1 min at 120 cycles/day (2 Hz) for 3 consecutive days at low, medium and high magnitude of strain, and sacrificed 16 days after initiation of loading [24]. Mice were injected with calcein (10 mg/kg) and alizarin

red (15 mg/kg) (Sigma Chemical Co, St. Louis, MO), 10 and 3 days before sacrifice, respectively, as previously described [23]. The left ulnae served as non-loaded internal controls.

To examine the effect of loading on sclerostin and Wnt target gene expression, bones were collected after a single loading bout for mRNA expression or after 2 loading bouts for protein expression. This approach assures that data represent early changes in gene expression induced by loading rather than changes due to alterations in bone cell populations. We have used these time points for sample collection in our earlier publication demonstrating changes in Sost and sclerostin expression [21]. For mRNA analysis by quantitative PCR, ulnae were loaded once at high strain magnitude and mice were sacrificed 24 h later. Bones were snap-frozen in liquid nitrogen and stored at −80°C until RNA isolation. For protein analyses by Western blotting and immunohistochemistry, mice were loaded for 2 consecutive days at high strain magnitude and sacrificed 24 h after the second loading bout. Ulnae were dissected and cleaned off soft tissue. Bones were snap-frozen in liquid nitrogen and stored at −80°C until used for preparation of protein lysates, or fixed in 10% buffered formalin and stored in 70% ethanol at 4°C until processed for immunohistochemistry.

Dynamic bone histomorphometry

Dynamic bone histomorphometric analysis was done as previously described [13]. Briefly, thick (100 μm) cross-sections at the mid-diaphysis of ulnae embedded in methyl methacrylate were prepared using a diamond embedded wire saw (Histosaw, Delaware Diamond Knives, Wilmington, DE) and ground to a final thickness of around 40 μm. Total, single, and double labeled perimeter, and inter-label width were measured on periosteal surfaces using a semiautomatic analysis system (Bioquant OSTEO 7.20.10, Bioquant Image Analysis Co., Nashville, TN) attached to a microscope equipped with an ultraviolet light source (Nikon Optiphot 2 microscope, Melville, NY). The terminology and units used are those recommended by the Histomorphometry Nomenclature Committee of the American Society for Bone and Mineral Research [25].

Quantitative PCR

Total RNA was extracted from ulnar mid-diaphysis (approximately 1/3 of the bone) using Ultraspec reagent (Biotecx Laboratories, Houston, TX) and treated with RNase-free DNase (Promega, Madison, WI). cDNA was synthesized using high capacity cDNA reverse transcription kit (Applied Biosystems, Foster City, CA). Gene expression was analyzed by quantitative PCR using primer probe sets from Applied Biosystems or from Roche Applied Science (Indianapolis, IN). Relative mRNA expression levels were normalized to the house-keeping gene ribosomal protein S2 (ChoB) using the ΔCt method.

Western blotting

Protein lysates were prepared from ulnar mid-diaphysis (approximately 1/3 of the bone), as previously described [15]. Twenty μg of protein were separated on a 10% SDS-PAGE gel and electrotransferred to PVDF membrane (Millipore, Billerica, MA). Immunoblots were performed using goat polyclonal anti-mouse sclerostin antibody (1:100 in 5% non fat milk, R&D Systems, Minneapolis, MN), which recognizes both murine and human sclerostin, or mouse monoclonal anti-α-tubulin antibody (1:2000 in 5% non-fat milk, Santa Cruz Biotechnology, Santa Cruz, CA), followed by rabbit anti-goat or goat anti-mouse antibodies, respectively, conjugated with horseradish peroxidase (1:2000 in 5% milk, Santa Cruz Biotechnology). Blots were developed using enhanced chemiluminescence (Pierce Biotechnology Inc., Rockford, IL). The intensity of the bands was quantified using NIH ImageJ (http://rsb.info.nih.gov/ij/).

Immunohistochemistry

Detection of sclerostin expression was performed on demineralized, paraffin embedded sections of ulnae mid-diaphysis, as previously described [13]. Briefly, bones were demineralized in 10% EDTA/4% phosphate buffered formalin (7:3) for 7 days at 4°C with agitation. Five-μm thick sections were cut and mounted to glass slides. Sections were deparaffinized, treated with 3% H_2O_2 to inhibit endogenous peroxidase activity, blocked with rabbit or goat serum, and then incubated with 1:100 dilution of the goat polyclonal anti-mouse sclerostin antibody used for Western blotting (R&D Systems, Minneapolis, MN). Sections were then incubated with rabbit anti-goat horseradish peroxidase-conjugated antibody (Santa Cruz Biotechnology, Santa Cruz, CA). Color was developed with a diaminobenzidine substrate chromogen system (Dako Corp., Carpinteria, CA). Non-immune IgGs were used as negative controls. 0.2% methyl green was used for counter stain. Sections were observed under an Olympus BX51TRF microscope (Olympus America Inc., Center Valley, PA) at 400× magnification. The number of sclerostin-positive osteocytes, defined as osteocyte cell bodies exhibiting brown staining, and sclerostin-negative osteocytes, defined as osteocyte cell bodies exhibiting methyl green staining, were quantified using the OsteoMeasure High Resolution Digital Video System (OsteoMetrics Inc., Decatur, GA). The percentage of sclerostin-positive cells was quantified in the medial region of the ulnae receiving high peak strain during loading, as previously described [21].

Measurement of human and murine sclerostin

Murine and human sclerostin levels were measured using species-specific custom-made single-plex Luminex kits (Millipore/Linco, St. Charles, MO). The standard range for the mouse sclerostin assay was of 5 pg/ml to 20 ng/ml with a limit of detection of 10 pg/ml; and the standard range for the human sclerostin assay was 12 pg/ml to 50 ng/ml down with a limit of detection of 15 pg/ml. For measurements of circulating sclerostin, sera were collected from transgenic and wild type littermate mice at 16 weeks of age before loading and 24 hours after 1 or 2 loading bouts at high strain magnitude. For the tissue measurements, femora and the 6^{th} lumbar vertebrae were removed at necropsy, snap-frozen in liquid nitrogen, and pulverized. Total protein was extracted with a digestion buffer (50 mM Tris buffer, pH 7.4, containing 0.1 M sodium chloride and 0.1% Triton X-100). Sclerostin levels detected in protein extracts were normalized to total protein concentration in lysates (determined by a BCA kit, Pierce Biotechnology, Inc., Rockford, IL).

Statistical Analysis

Data were analyzed using SigmaStat (SPSS Science, Chicago, IL). All values are reported as the mean ± standard deviations (SD). Differences between wild type and transgenic mice were evaluated using Student's t-Test. Differences between loaded and non-loaded groups for each genotype were evaluated by paired t-Test. A p value of 0.05 or lower was considered statistically significant.

Results

Transgenic mice overexpressing human *SOST* in osteocytes (DMP1-*SOST*) exhibit low bone mass in the axial skeleton, but no changes in mass or geometry of long bones

In a previous study, we showed that DMP1-*SOST* mice exhibit a marked decrease in BMD in the spine with minimal if any changes in the long bones at 8 weeks of age [13]. Consistent with these earlier findings, longitudinal analysis of a cohort of DMP1-*SOST* mice and control littermates from 4 to 16 weeks of age demonstrated a progressive decrease in BMD in the lumbar spine and total body BMD in both female and male mice (Table 1). A transient decrease in femoral BMD was observed at 4 weeks of age in females and at 4 and 8 weeks

of age in males. However, by 16 weeks of age femoral BMD in DMP1-*SOST* mice was not different from littermate controls in either sex. No difference in body weight was found at any age.

Micro-CT analysis showed a dramatic decrease in BV/TV, trabecular number, trabecular thickness, and trabecular separation in cancellous bone of the spine of DMP1-*SOST* compared to wild type mice at 6 and 10 weeks of age (Table 2). In contrast, no changes were observed in tissue area, bone area, marrow area, cross-sectional thickness, or minimum second moment of area (Imin) in cortical bone of the femoral or ulnar bones (Tables 2 and 3). Material density, which indicates the degree of bone mineralization, was not different in either cancellous or cortical bone in DMP1-*SOST* mice compared to wild type littermates. No differences in the length of femur or tibia were found between wild type and transgenic mice (Table 3).

Loading decreased endogenous murine *Sost* expression, but did not alter the expression of the human *SOST* transgene

Despite the lack of detectable differences in bone area, geometry, or mineralization, ulnae from DMP1-*SOST* mice were more compliant to *ex vivo* cyclic axial loading. Thus, the same loading force generated higher strains in DMP1-*SOST* mice compared to wild type littermates (Figure 1A and B). Based on these measurements, right ulnae from wild type and DMP1-*SOST* mice were subjected to *in vivo* loading by applying appropriate forces required to induce equivalent strains of low, medium, and high magnitude (Figure 1C). WT mice were loaded at 2.20 N, 2.56 N, and 2.90 N for low, medium, and high mechanical stimulation, respectively. To generate equivalent strain in the TG mice at each load level, 1.90 N, 2.20 N, and 2.50 N were used for low, medium, and high mechanical stimulation, respectively.

Consistent with earlier findings [21], loading decreased *Sost* mRNA and sclerostin protein expression measured 24 h after 1 or 2 loading bouts at high strain, respectively, in wild type mice (Figure 2A, B, and C). A similar decrease in murine (endogenous) *Sost* mRNA was induced by loading in DMP1-*SOST* mice (Figure 2A). In contrast, the expression of human *SOST* mRNA, which was only detectable in bones of transgenic mice, was not affected by loading. This result demonstrates that the 8kb fragment of the DMP1 promoter is not regulated by mechanical stimulation, unlike the endogenous DMP1 gene that is upregulated [26]. Likewise, sclerostin expression, quantified by Western blotting using an antibody that recognizes both murine and human sclerostin, was not decreased by loading in the transgenic mice (Figure 2B). Loading significantly reduced the number of sclerostin-positive osteocytes in wild type mice, but not in transgenic mice, as assessed by immunohistochemistry using the same antibody (Figure 2C). To discriminate between the murine and human proteins, sclerostin was quantified in serum and bone tissue using species-specific Luminex assays. In contrast to the decrease in *Sost* and sclerostin expression induced by loading in bone, circulating levels of murine sclerostin were not changed by loading in wild type or transgenic mice of either sex (Figure 2D). Human sclerostin was not detected in serum of transgenic mice, likely due to levels below the sensitivity of the assay. However, detectable levels of the human protein were found in bones of transgenic mice of both sexes at concentrations about ten times lower than the murine sclerostin (Figure 2E). As previously shown at the mRNA level [13], the expression of endogenous murine sclerostin protein was similar in transgenic and wild type mice. No changes in osteocyte number or osteocyte density were found in DMP1-*SOST* mice compared to wild type littermates or in either type of mice under non-loaded and loaded conditions (not shown).

Overexpression of *SOST*/sclerostin in osteocytes disrupted the osteogenic response to mechanical stimulation

To test whether the inability to downregulate the human *SOST* transgene affected the osteogenic response induced by mechanical stimulation, bone formation was measured in DMP1-*SOST* mice and wild type littermates subjected to ulnae loading. Bones from wild type mice exhibited a robust and dose-responsive increase in osteogenesis as a result of cyclic axial loading, as revealed by increased fluorochrome incorporation on the periosteal surface (Figure 3A). However, fluorochrome incorporation in loaded arms from transgenic mice was not significantly different from the contralateral (non-loaded) control limb. Quantification of bone formation indices in non-loaded ulnae showed no differences between wild type and transgenic mice in basal mineralizing surface per bone surface (MS/BS), mineral apposition rate (MAR), or the resulting bone formation rate per bone surface (BFR/BS) (Figure 3B). In wild type mice, loading induced the expected strain-dependent increase in MS/BS and MAR, representing the surface covered by osteoblasts and the work of osteoblasts, respectively. This resulted in a marked increase in BFR/BS. In contrast, load-induced MS/BS was greatly reduced, and the increase in MAR was abolished in transgenic mice, resulting in a dramatic blunting in BFR/BS with only a minimal increase induced by high strain loading (Figure 3B). Overexpression of human *SOST* in osteocytes caused a 70–85% reduction in relative BFR, calculated as BFR/BS in the loaded ulnae minus BFR/BS in the control non-loaded ulnae per unit strain, compared to wild type mice (Figure 3C). This demonstrates that bones from transgenic mice exhibit an overall reduced sensitivity to mechanical loading.

Overexpression of *SOST*/sclerostin in osteocytes suppressed the activation of Wnt signaling induced by mechanical stimulation

As expected, loading increased mRNA transcripts of several genes associated with activation of Wnt signaling [23, 27], measured 24 h after 1 loading bout at high strain in wild type mice (Figure 4A). However, the effect of loading on Wnt target gene expression was absent in DMP1-*SOST* transgenic mice. Consistent with the antagonism of the Wnt signaling pathway attributed to sclerostin, basal levels of some of the Wnt target genes, i.e. BMP4, Smad6, naked2, and connexin 43, were significantly decreased in bones of transgenic mice compared to wild type littermates.

Moreover, loading increased the expression of Osterix and collagen1a1 in wild type mice (Figure 4B). In addition, it increased Runx2 and osteocalcin; and, although changes were not statistically significant by paired t-Test, they were close to become significant or reached significance, respectively, by Student t-Test. In contrast, loading did not significantly affect the expression of these genes in DMP1-*SOST* transgenic mice. Furthermore, DMP1-*SOST* mice exhibit increased basal levels of Runx2 and Osterix, as well as the early osteoblast marker collagen1a1, suggesting a potential interference with the late stages of osteoblast differentiation by sclerostin.

Discussion

Although it has been long recognized that mechanical loading stimulates new bone formation on surfaces adjacent to areas to which strain is applied [20, 28], the cellular and molecular mechanism(s) responsible for this phenomenon still remains unclear. Earlier studies demonstrated that loading reduces the expression of sclerostin, the bone formation inhibitor encoded by the *Sost* gene, in osteocytes located close to high bone formation surfaces [21], and that activation of the Wnt pathway is one of the earliest responses of bone to mechanical stimulation [27, 29]. Based on this previous evidence, we investigated here whether downregulation of sclerostin expression in osteocytes was a prerequisite for

osteogenesis induced by mechanical stimulation. Using a mouse model in which the human *SOST* is expressed in osteocytes and is not regulated by loading, we provide conclusive evidence that reduction of sclerostin is necessary for stimulation of the expression of Wnt target genes and the increase in bone formation induced by mechanical force.

The mechanism by which sclerostin inhibits bone formation is not completely understood. The current knowledge indicates that sclerostin binds to LRP6 and LRP5, transmembrane proteins that together with frizzled receptors mediate the actions of Wnts [30, 31]. This event, in turn, interferes with signaling downstream of the receptors, thereby antagonizing the pro-differentiating and survival effects of Wnts on cells of the osteoblastic lineage [32, 33]. Consistent with previously reported Sost overexpressing mice [11, 12], DMP1-*SOST* mice exhibit a stronger osteopenic phenotype in the axial compared to the appendicular skeleton. This difference might be due to a higher impact of overexpressing *SOST* and reducing Wnt signaling in cancellous bone, which exhibits higher remodeling rate than cortical bone and is the major contributor to bone mass in the spine. In spite of lack of a basal phenotype in the long bones, the response to loading in the ulnae was markedly reduced in DMP1-*SOST* mice. Moreover, the relatively small increases in human transgenic sclerostin levels were sufficient to abrogate the anabolic response, even if they apparently do not fully compensate for the reduction in the endogenous protein induced by loading. These findings suggest that there is a threshold of sclerostin above which bone formation is inhibited, rather than a linear relationship between sclerostin and bone formation.

Similar to our findings with the DMP1-*SOST* transgenic mice, the response to mechanical loading is greatly reduced in mice with germ line deletion of LRP5 [24]. Thus, either overexpression of the Wnt antagonist sclerostin in bone or absence of the LRP5 Wnt co-receptor gene dampens the anabolic response to mechanical force. Recent evidence has challenged the role of LRP5 function in bone cells by proposing that LRP5 signaling increases bone formation through inhibition of serotonin synthesis in the duodenum [34]. However, a more recent report failed to detect an association between bone formation directed by LRP5 signaling and systemic effects mediated by serotonin. Rather, LRP5 was found to function in bone (particularly, in osteocytes) to regulate bone mass [35]. Our findings demonstrating that loading decreases sclerostin expression in bone without affecting circulating levels of the protein in wild type mice argue against an extra-skeletal effect of mechanical loading through sclerostin. Moreover, human sclerostin is only detected in bone but not in serum of DMP1-*SOST* transgenic mice, likely due to its ~10-times lower expression in bone compared to the murine endogenous protein, suggesting that human sclerostin does not reach the circulation at high enough levels to potentially induce a systemic response in other tissues. In particular, we have shown that DMP1-*SOST* mice do not exhibit higher intestinal levels of expression of Tph1 [13], the enzyme that controls serotonin synthesis, as would be expected if sclerostin would have interfered with LRP5 signaling in the gut. Thus, the inability of loading to increase bone formation in DMP1-*SOST* mice can be attributed solely to the local increase in human sclerostin that is not down-regulated by mechanical force.

Systemic elevation of PTH also decreases sclerostin expression [15, 16], and transgenic mice expressing a constitutively active PTH receptor specifically in osteocytes (DMP1-caPTHR1 mice) exhibit reduced sclerostin levels [13, 23]. Moreover, the elevated rate of periosteal bone formation in these mice is prevented in double transgenic mice also expressing the human *SOST* gene in osteocytes (DMP1-caPTHR1;DMP1-*SOST* mice) [13]. Taken together with the current findings, this evidence indicates that hormonal and mechanical stimuli converge in downregulation of sclerostin expression, leading to either systemic or local regulation of bone formation.

The process of mechanotransduction is complex and likely results from concerted contributions of diverse molecular cascades activated by mechanical stimuli in bone cells. Consistent with this notion, altered responses to loading are exhibited by mice with ubiquitous or osteoblast/osteocyte-specific deletion of genes involved in different signaling pathways, including LRP5 [24, 36], the estrogen receptors α and β [37, 38], purinergic receptor P2X7 [39], polycystin-1 [40] and connexin 43 [41]. The defective response to loading in these models could be due to a failure of the osteocytes to sense mechanical stimuli that reach the bone or to transmit signals leading to increase bone formation; or to an impaired synthetic activity of the osteoblasts. The current studies demonstrate that precluding osteocytes from transmitting mechanical signals through downregulation of sclerostin results in failure of osteoblasts to respond to loading by increasing Wnt signaling and enhancing bone formation. Thus, mechanotransduction necessitates local regulation of Wnt signaling directed by osteocytes.

Research highlights

- The osteocyte network might detect variations in the level of mechanical strain and distribute signals leading to adaptive responses.
- Loading downregulates the bone formation inhibitor and Wnt antagonist *Sost*/sclerostin in osteocytes adjacent to high bone formation surfaces.
- We used DMP1-8kb-SOST mice, in which human SOST is expressed in osteocytes and it is not decreased by loading.
- Maintaining high sclerostin expression in DMP1-8kb-SOST mice prevented Wnt activation and the increase in bone formation induced by loading.
- Thus, mechanotransduction necessitates sclerostin reduction in osteocytes to direct Wnt signaling and osteogenesis to where bone is needed.

Abbreviations

DMP1	dentin matrix protein 1
PTHrP	PTH related protein
BMP	bone morphogenetic protein
Cx43	connexin 43
WT	wild type
TG	transgenic mice
ChoB	ribosomal protein S2
LRP	low density lipoprotein receptor-related protein
Tph1	Tryptophan hydroxylase 1

Acknowledgments

The authors thank R. Lee and J.D. Benson for technical assistance. This research was supported by the National Institutes of Health (R01DK076007 and an American Recovery and Reinvestment Act supplement).

References

1. Wolff, J. Das gesetz der transformation der knochen (The law of bone remodeling). Berlin: Springer-Verlag; 1892.
2. Frost HM. The mechanostat: a proposed pathogenic mechanism of osteoporoses and the bone mass effects of mechanical and nonmechanical agents. Bone Miner. 1987; 2:73–85. [PubMed: 3333019]
3. Martin, RB.; Burr, DB.; Sharkey, NA. Skeletal tissue mechanics. New York: Springer-Verlag; 1998.
4. Bonewald LF, Johnson ML. Osteocytes, mechanosensing and Wnt signaling. Bone. 2008; 42:606–615. [PubMed: 18280232]
5. Aarden EM, Burger EH, Nijweide PJ. Function of osteocytes in bone. J. Cell. Biochem. 1994; 55:287–299. [PubMed: 7962159]
6. Paszty C, Turner CH, Robinson MK. Sclerostin: a gem from the genome leads to bone-building antibodies. J. Bone Miner. Res. 2010; 25:1897–1904. [PubMed: 20564241]
7. Balemans W, Ebeling M, Patel N, Van Hul E, Olson P, Dioszegi M, Lacza C, Wuyts W, Van Den Ende J, Willems P, Paes-Alves AF, Hill S, Bueno M, Ramos FJ, Tacconi P, Dikkers FG, Stratakis C, Lindpaintner K, Vickery B, Foernzler D, Van Hul W. Increased bone density in sclerosteosis is due to the deficiency of a novel secreted protein (SOST). Hum. Mol. Genet. 2001; 10:537–543. [PubMed: 11181578]
8. Brunkow ME, Gardner JC, Van Ness J, Paeper BW, Kovacevich BR, Proll S, Skonier JE, Zhao L, Sabo PJ, Fu Y, Alisch RS, Gillett L, Colbert T, Tacconi P, Galas D, Hamersma H, Beighton P, Mulligan J. Bone dysplasia sclerosteosis results from loss of the SOST gene product, a novel cystine knot-containing protein. Am. J Hum. Genet. 2001; 68:577–589. [PubMed: 11179006]
9. Li X, Ominsky MS, Niu QT, Sun N, Daugherty B, D'Agostin D, Kurahara C, Gao Y, Cao J, Gong J, Asuncion F, Barrero M, Warmington K, Dwyer D, Stolina M, Morony S, Sarosi I, Kostenuik PJ, Lacey DL, Simonet WS, Ke HZ, Paszty C. Targeted deletion of the sclerostin gene in mice results in increased bone formation and bone strength. J. Bone Miner. Res. 2008; 23:860–869. [PubMed: 18269310]
10. Lin C, Jiang X, Dai Z, Guo X, Weng T, Wang J, Li Y, Feng G, Gao X, He L. Sclerostin mediates bone response to mechanical unloading through antagonizing Wnt/beta-catenin signaling. J. Bone Miner. Res. 2009; 24:1651–1661. [PubMed: 19419300]
11. Winkler DG, Sutherland MK, Geoghegan JC, Yu C, Hayes T, Skonier JE, Shpektor D, Jonas M, Kovacevich BR, Staehling-Hampton K, Appleby M, Brunkow ME, Latham JA. Osteocyte control of bone formation via sclerostin, a novel BMP antagonist. EMBO J. 2003; 22:6267–6276. [PubMed: 14633986]
12. Loots GG, Kneissel M, Keller H, Baptist M, Chang J, Collette NM, Ovcharenko D, Plajzer-Frick I, Rubin EM. Genomic deletion of a long-range bone enhancer misregulates sclerostin in Van Buchem disease. Genome Res. 2005; 15:928–935. [PubMed: 15965026]
13. Rhee Y, Allen MR, Condon K, Lezcano V, Ronda AC, Galli C, Olivos N, Passeri G, O'Brien CA, Bivi N, Plotkin LI, Bellido T. PTH receptor signaling in osteocytes governs periosteal bone formation and intra-cortical remodeling. J. Bone Miner. Res. 2011; 26:1035–1046. [PubMed: 21140374]
14. Jilka RL. Inhibiting the inhibitor: a new route to bone anabolism. J. Bone Miner. Res. 2009; 24:575–577. [PubMed: 19335216]
15. Bellido T, Ali AA, Gubrij I, Plotkin LI, Fu Q, O'Brien CA, Manolagas SC, Jilka RL. Chronic elevation of PTH in mice reduces expression of sclerostin by osteocytes: a novel mechanism for hormonal control of osteoblastogenesis. Endocrinology. 2005; 146:4577–4583. [PubMed: 16081646]
16. Keller H, Kneissel M. SOST is a target gene for PTH in bone. Bone. 2005; 37:148–158. [PubMed: 15946907]
17. van Lierop AH, Witteveen J, Hamdy N, Papapoulos S. Patients with primary hyperparathyroidism have lower circulating sclerostin levels than euparathyroid controls. Eur. J. Endocrinol. 2010; 163:833–837. [PubMed: 20817762]
18. Drake MT, Srinivasan B, Modder UI, Peterson JM, McCready LK, Riggs BL, Dwyer D, Stolina M, Kostenuik P, Khosla S. Effects of parathyroid hormone treatment on circulating sclerostin

levels in postmenopausal women. J. Clin. Endocrinol. Metab. 2010; 95:5056–5062. [PubMed: 20631014]

19. Mirza FS, Padhi ID, Raisz LG, Lorenzo JA. Serum sclerostin levels negatively correlate with parathyroid hormone levels and free estrogen index in postmenopausal women. J. Clin. Endocrinol. Metab. 2010; 95:1991–1997. [PubMed: 20156921]
20. Robling AG, Turner CH. Mechanotransduction in bone: genetic effects on mechanosensitivity in mice. Bone. 2002; 31:562–569. [PubMed: 12477569]
21. Robling AG, Niziolek PJ, Baldridge LA, Condon KW, Allen MJ, Alam I, Mantila SM, Gluhak-Heinrich J, Bellido T, Harris SE, Turner CH. Mechanical stimulation of bone in vivo reduces osteocyte expression of Sost/sclerostin. J. Biol. Chem. 2008; 283:5866–5875. [PubMed: 18089564]
22. Kalajzic I, Braut A, Guo D, Jiang X, Kronenberg MS, Mina M, Harris MA, Harris SE, Rowe DW. Dentin matrix protein 1 expression during osteoblastic differentiation, generation of an osteocyte GFP-transgene. Bone. 2004; 35:74–82. [PubMed: 15207743]
23. O'Brien CA, Plotkin LI, Galli C, Goellner J, Gortazar AR, Allen MR, Robling AG, Bouxsein M, Schipani E, Turner CH, Jilka RL, Weinstein RS, Manolagas SC, Bellido T. Control of bone mass and remodeling by PTH receptor signaling in osteocytes. PLoS ONE. 2008; 3:e2942. [PubMed: 18698360]
24. Sawakami K, Robling AG, Ai M, Pitner ND, Liu D, Warden SJ, Li J, Maye P, Rowe DW, Duncan RL, Warman ML, Turner CH. The WNT co-receptor LRP5 is essential for skeletal mechanotransduction, but not for the anabolic bone response to parathyroid hormone treatment. J. Biol. Chem. 2006; 281:23698–23711. [PubMed: 16790443]
25. Parfitt AM, Drezner MK, Glorieux FH, Kanis JA, Malluche H, Meunier PJ, Ott SM, Recker RR. Bone histomorphometry: standardization of nomenclature, symbols, and units. J. Bone Min. Res. 1987; 2:595–610.
26. Yang W, Lu Y, Kalajzic I, Guo D, Harris MA, Gluhak-Heinrich J, Kotha S, Bonewald LF, Feng JQ, Rowe DW, Turner CH, Robling AG, Harris SE. Dentin matrix protein 1 gene cis-regulation: use in osteocytes to characterize local responses to mechanical loading *in vitro* and *in vivo*. J. Biol. Chem. 2005; 280:20680–20690. [PubMed: 15728181]
27. Robinson JA, Chatterjee-Kishore M, Yaworsky PJ, Cullen DM, Zhao W, Li C, Kharode Y, Sauter L, Babij P, Brown EL, Hill AA, Akhter MP, Johnson ML, Recker RR, Komm BS, Bex FJ. WNT/beta-catenin signaling is a normal physiological response to mechanical loading in bone. J. Biol. Chem. 2006; 281:31720–31728. [PubMed: 16908522]
28. Burr DB, Robling AG, Turner CH. Effects of biomechanical stress on bones in animals. Bone. 2002; 30:781–786. [PubMed: 11996920]
29. Hens JR, Wilson KM, Dann P, Chen X, Horowitz MC, Wysolmerski JJ. TOPGAL mice show that the canonical Wnt signaling pathway is active during bone development and growth and is activated by mechanical loading *in vitro*. J. Bone Miner. Res. 2005; 20:1103–1113. [PubMed: 15940363]
30. Li X, Zhang Y, Kang H, Liu W, Liu P, Zhang J, Harris SE, Wu D. Sclerostin binds to LRP5/6 and antagonizes canonical Wnt signaling. J. Biol. Chem. 2005; 280:19883–19887. [PubMed: 15778503]
31. Van Bezooijen RL, Roelen BA, Visser A, Wee-Pals L, de Wilt E, Karperien M, Hamersma H, Papapoulos SE, Ten Dijke P, Lowik CW. Sclerostin ss an osteocyte-expressed negative regulator of bone formation, but not a classical BMP antagonist. J Exp. Med. 2004; 199:805–814. [PubMed: 15024046]
32. Glass DA, Karsenty G. In vivo analysis of Wnt signaling in bone. Endocrinology. 2007; 148:2630–2634. [PubMed: 17395705]
33. Baron R, Rawadi G. Targeting the Wnt/beta-catenin pathway to regulate bone formation in the adult skeleton. Endocrinology. 2007; 148:2635–2643. [PubMed: 17395698]
34. Yadav VK, Ryu JH, Suda N, Tanaka KF, Gingrich JA, Schutz G, Glorieux FH, Chiang CY, Zajac JD, Insogna KL, Mann JJ, Hen R, Ducy P, Karsenty G. Lrp5 controls bone formation by inhibiting serotonin synthesis in the duodenum. Cell. 2008; 135:825–837. [PubMed: 19041748]

35. Cui Y, Niziolek PJ, MacDonald BT, Zylstra CR, Alenina N, Robinson DR, Zhong Z, Matthes S, Jacobsen CM, Conlon RA, Brommage R, Liu Q, Mseeh F, Powell DR, Yang Q, Zambrowicz B, Gerrits H, Gossen JA, Hec X, Bader M, Williams BO, Warman ML, Robling AG. LRP5 functions in bone to regulate bone mass. Nature Medicine. 2011; 17:684–691.

36. Saxon LK, Jackson BF, Sugiyama T, Lanyon LE, Price JS. Analysis of multiple bone responses to graded strains above functional levels, and to disuse, in mice in vivo show that the human Lrp5 G171V High Bone Mass mutation increases the osteogenic response to loading but that lack of Lrp5 activity reduces it. Bone. 2011 in press.

37. Lee KC, Jessop H, Suswillo R, Zaman G, Lanyon LE. The adaptive response of bone to mechanical loading in female transgenic mice is deficient in the absence of oestrogen receptor-alpha and -beta. J. Endocrinol. 2004; 182:193–201. [PubMed: 15283680]

38. Lee K, Jessop H, Suswillo R, Zaman G, Lanyon L. Endocrinology: bone adaptation requires oestrogen receptor-alpha. Nature. 2003; 424:389. [PubMed: 12879058]

39. Li J, Liu D, Ke HZ, Duncan RL, Turner CH. The P2X7 nucleotide receptor mediates skeletal mechanotransduction. J. Biol. Chem. 2005; 280:42952–42959. [PubMed: 16269410]

40. Xiao Z, Dallas M, Qiu N, Nicolella D, Cao L, Johnson M, Bonewald L, Quarles LD. Conditional deletion of Pkd1 in osteocytes disrupts skeletal mechanosensing in mice. FASEB J. 2011; 25:2418–2432. [PubMed: 21454365]

41. Grimston SK, Brodt MD, Silva MJ, Civitelli R. Attenuated response to in vivo mechanical loading in mice with conditional osteoblast ablation of the Connexin43 gene (Gja1). J. Bone Miner. Res. 2008; 23:879–886. [PubMed: 18282131]

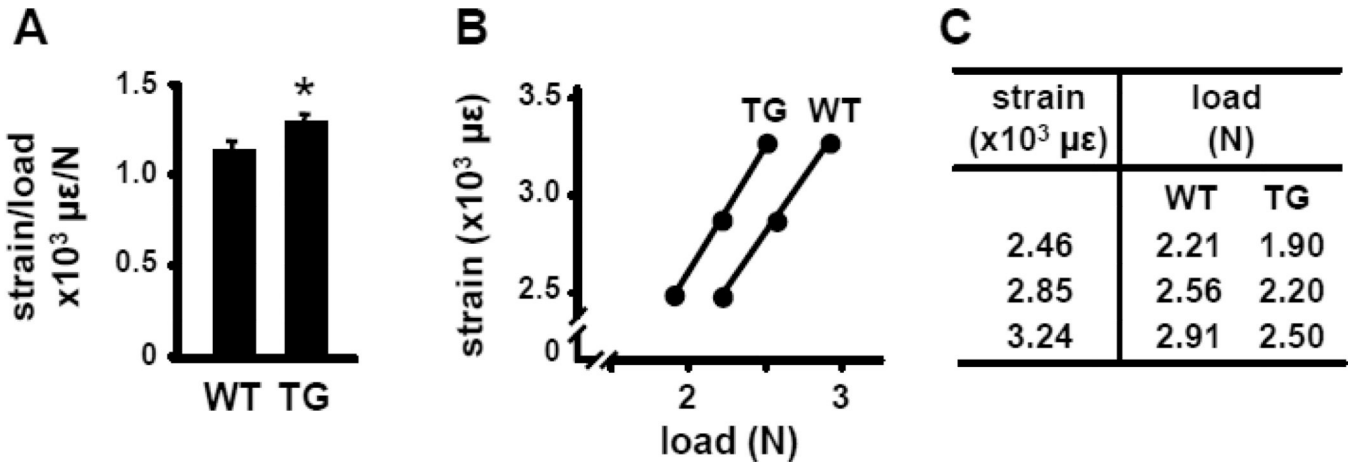

C

strain ($x10^3$ με)	load (N)	
	WT	TG
2.46	2.21	1.90
2.85	2.56	2.20
3.24	2.91	2.50

Figure 1. DMP1-*SOST* mice exhibit less resistance to mechanical loading

A. *Ex vivo* strain measurements were performed at the medial surface of the ulnar midshaft from WT and TG mice. TG mice exhibited greater deformation per unit force than their WT counterparts. Bars represent means ± SD, n=6. * indicates $p<0.05$ versus WT mice by Student's t-Test. **B**. Linear relation between applied peak force and mechanical strain in the midshaft ulna from WT and TG mice. **C**. Loading forces applied to achieve equivalent low, medium, and high magnitude of strain in WT and TG ulnae are shown.

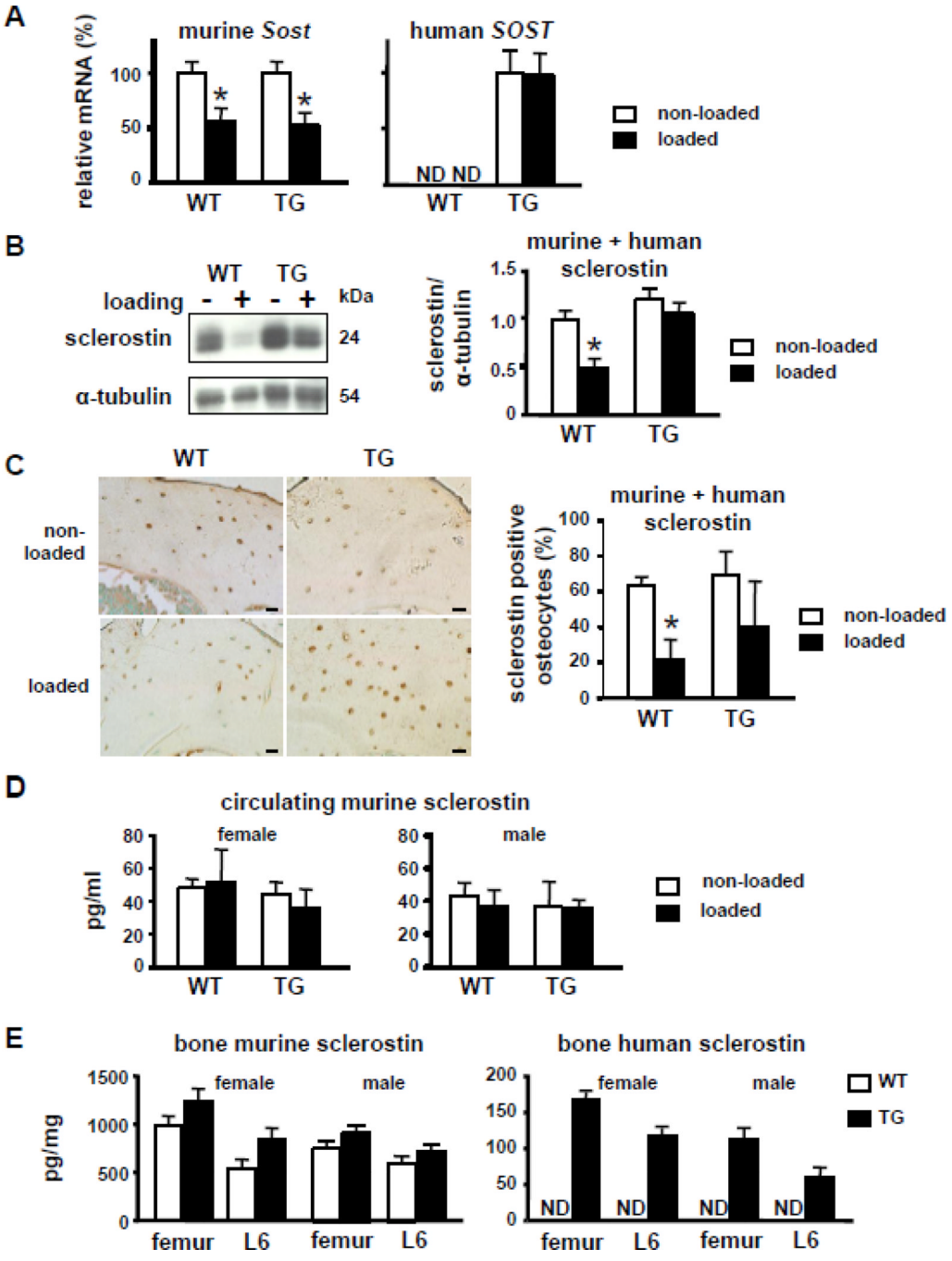

Figure 2. Loading decreases endogenous murine *Sost* expression, but does not alter the expression of the human *SOST* transgene in bone

A *Sost* mRNA expression in ulnae from WT and TG mice loaded at high magnitude strain was normalized to ChoB expression. Values are expressed as percentage of non-loaded ulnae for each genotype. n=3. **B**. Sclerostin expression in protein extracts from control and loaded ulnae of WT and TG mice was measured by Western blotting using an antibody that recognizes murine and human sclerostin. Representative images of one mouse per genotype are shown. Sclerostin expression was normalized to α-tubulin. n=3. **C**. Bone sections were stained with the same antibody used in the Western blot analysis. Representative images of one mouse per genotype are shown. Bars indicate 20 μm. Osteocytes expressing sclerostin

were enumerated in the medial region of the ulnae. Results are expressed as percent of the total number of osteocytes. n=3. **D** and **E**. Murine and human sclerostin protein levels were measured in the sera or bones (femur and the 6^{th} lumbar vertebra, L6) from WT and TG mice. n= 5–9 per group. Bars represent means ± SD. ND, not detected. * indicates $p<0.05$ versus non-loaded ulnae of the corresponding genotype by paired t-Test.

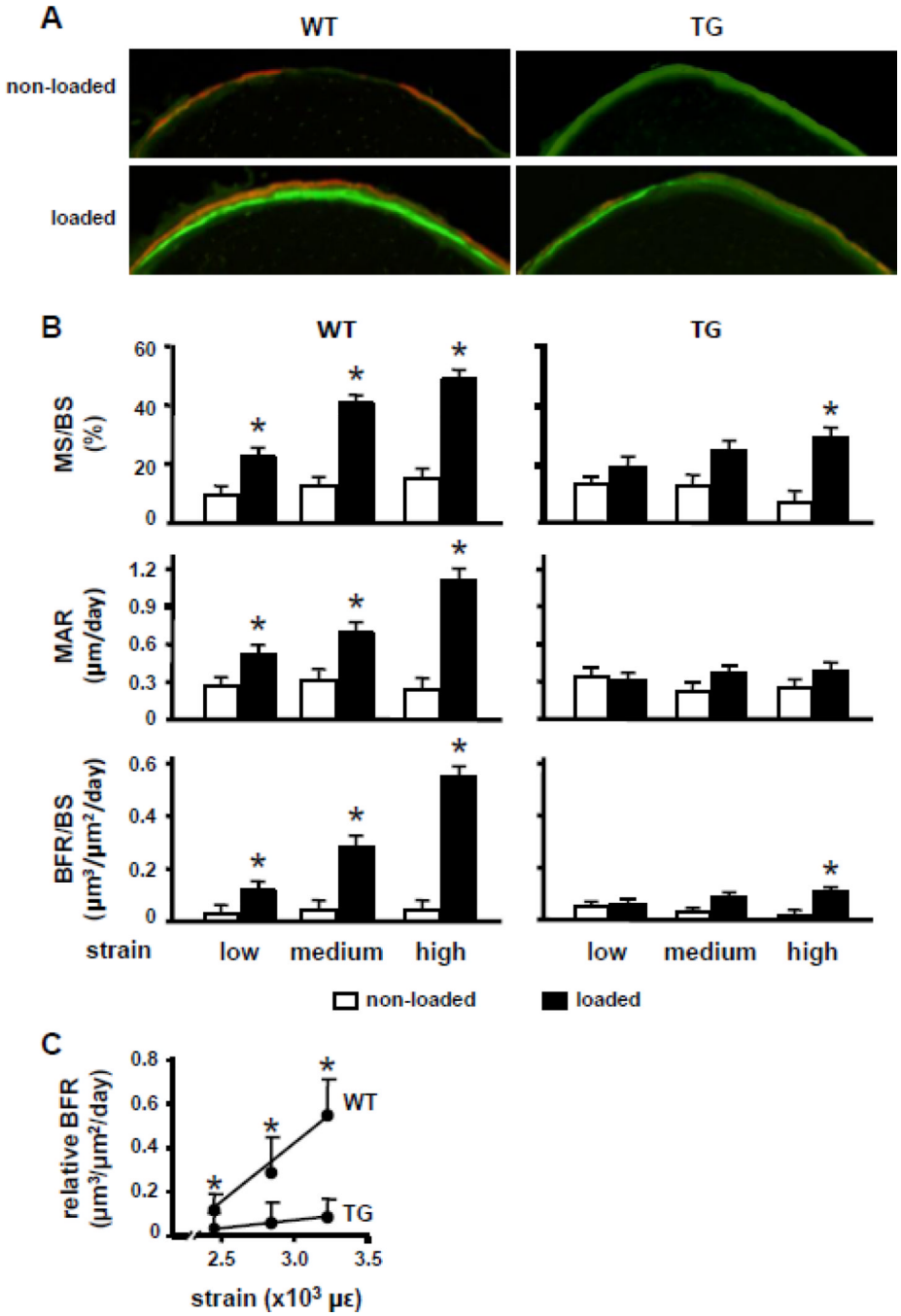

Figure 3. *SOST* overexpression in osteocytes markedly impairs the osteogenic response to loading

A. Representative images from the medial ulnar cortex of WT and TG mice that underwent high-magnitude loading. Note the extensive fluorochrome labeling and large interlabel width in the loaded ulna from the WT mouse, contrasted with the weak labeling and minimal (barely detectable) interlabel width in the loaded ulna from the TG mouse. **B**. Bone histomorphometric measurements were performed on control and loaded ulnae at low, medium, and high magnitude of strain. MS/BS, percent mineralizing bone surface per bone surface; MAR, mineral apposition rate; BFR/BS, bone formation rate per bone surface. Bars represent means ± SD, n=6–8. *p<0.05 versus non-loaded ulnae of the corresponding

genotype, by paired t-Test. **C**. Relative bone formation rate, BFR/BS of loaded minus non-loaded ulnae for each mouse at each strain magnitude. Means and SD are shown. n=6–8. * indicates $p<0.05$ versus TG mice by Student's t-Test.

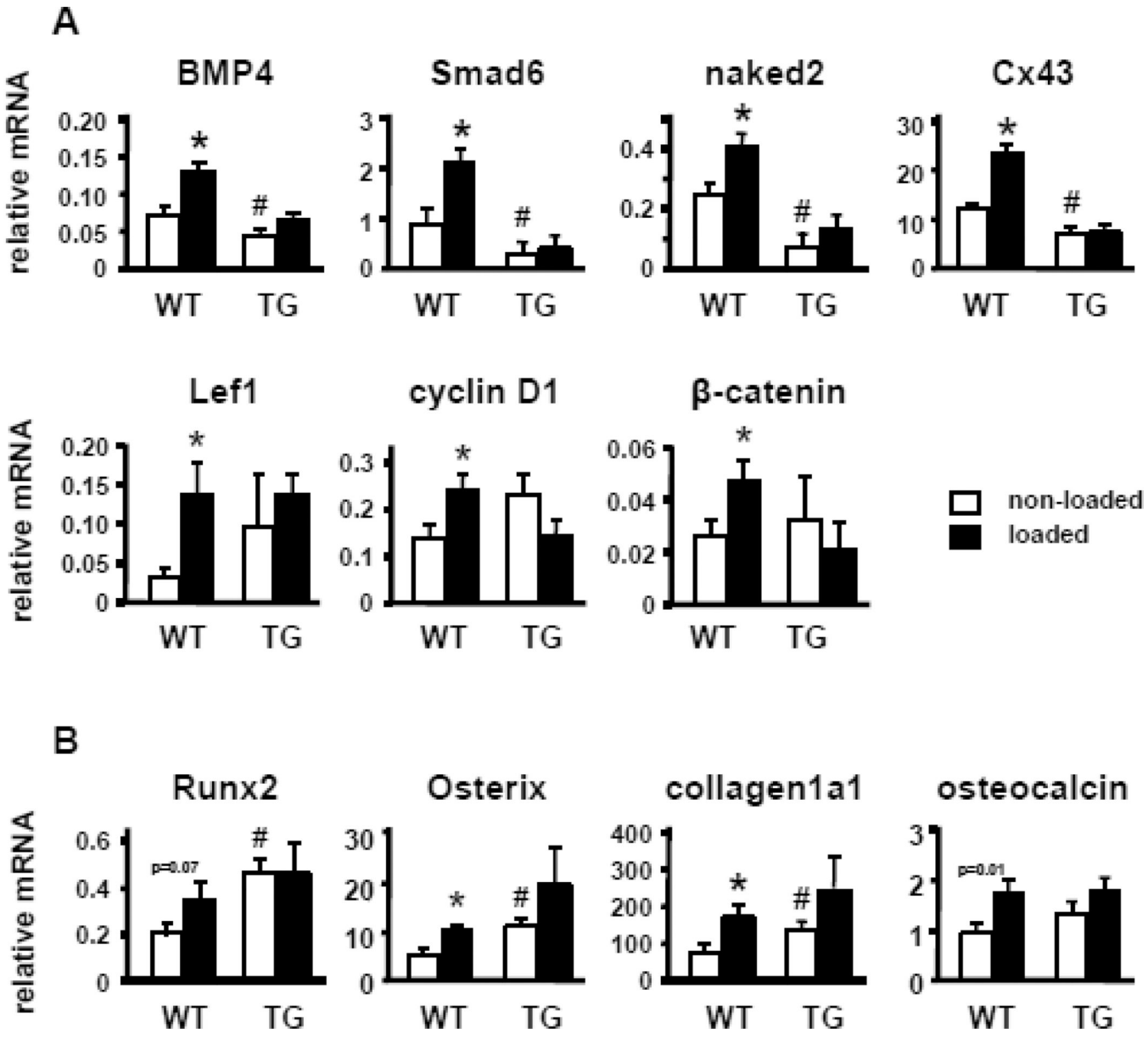

Figure 4. *SOST* overexpression in osteocytes inhibits basal and load-induced activation of Wnt signaling

Wnt target genes and osteoblast markers were measured by quantitative PCR and normalized to ChoB expression, in control and loaded ulnae of WT and TG mice. Bars represent means ± SD, n=3. * indicates $p<0.05$ versus the corresponding non-loaded mice by paired t-Test. # indicates $p<0.05$ versus non-loaded WT mice by Student's t-Test. P values indicated for Runx2 and OCN correspond to Student's t-Test analysis.

Table 1

Transgenic mice overexpressing human *SOST* in osteocytes exhibit low bone mass in the axial skeleton, but no changes in mass of long bones

age	**4-week-old**		**8-week-old**		**16-week-old**	
	WT	**TG**	**WT**	**TG**	**WT**	**TG**
body weight (g), female	14.8 ± 1.2	15.1 ± 1.2	19.7 ± 1.3	20.2 ± 1.3	21.9 ± 1.5	21.5 ± 0.7
n	8	9	8	9	6	5
body weight (g), male	17.4 ± 1.2	17.1 ± 1.5	23.7 ± 1.3	22.4 ± 1.7	26.2 ± 2.5	26.4 ± 3.0
n	6	12	6	12	6	6
BMD (mg/cm^2), female	WT	TG	WT	TG	WT	TG
total	33 ± 1	31 ± 1*	44 ± 1	42 ± 1*	50 ± 2	48 ± 2
femoral	42 ± 2	41 ± 1*	61 ± 2	60 ± 2	66 ± 1	66 ± 2
spinal	36 ± 2	33 ± 2*	48 ± 2	45 ± 2*	59 ± 3	53 ± 4*
n	8	9	8	9	6	5
BMD (mg/cm^2), male	WT	TG	WT	TG	WT	TG
total	34 ± 1	31 ± 1*	44 ± 1	41 ± 1*	49 ± 2	48 ± 2
femoral	45 ± 2	41 ± 3*	63 ± 3	60 ± 3*	72 ± 4	69 ± 2
spinal	36 ± 1	32 ± 1*	48 ± 1	43 ± 2*	56 ± 4	48 ± 3*
n	6	12	6	12	6	6

Values are means ± SD.

*p<0.05 versus WT mice by Student's t-Test.

Table 2

DMP1-*SOST* transgenic mice exhibit low cancellous bone volume, but no changes in volume or geometry of cortical bone

bone	parameters	unit	female (6-week-old)		male (6-week-old)		mixed gender (10-week-old)	
			WT	TG	WT	TG	WT	TG
spine (L3) (cancellous)	BV/TV	%	17.17 ± 1.13	6.62 ± 0.69*	19.37 ± 0.73	9.71 ± 2.70*	25.49 ± 2.34	9.54 ± 2.95*
	Tb.No.	1/mm	4.45 ± 0.32	1.56 ± 0.16*	4.84 ± 0.17	2.19 ± 0.46*	5.14 ± 0.20	1.52 ± 0.37*
	Tb.Th.	mm	0.0386 ± 0.0004	0.0425 ± 0.0022*	0.040 ± 0.001	0.044 ± 0.003*	0.050 ± 0.005	0.062 ± 0.005*
	Tb.Sp.	mm	0.14 ± 0.01	0.23 ± 0.01*	0.129 ± 0.002	0.20 ± 0.02*	0.15 ± 0.02	0.30 ± 0.08*
	Ma.D.	pixel	145.58 ± 1.68	144.85 ± 4.51	142.94 ± 2.56	147.61 ± 6.64	130.12 ± 5.54	136.29 ± 4.49
femur diaphysis (cortical)	T.Ar.	mm^2	1.65 ± 0.10	1.66 ± 0.03	1.92 ± 0.30	1.86 ± 0.31	1.77 ± 0.01	2.07 ± 0.33
	B.Ar.	mm^2	0.46 ± 0.04	0.46 ± 0.03	0.63 ± 0.06	0.63 ± 0.12	0.77 ± 0.09	0.84 ± 0.13
	M.Ar.	mm^2	1.20 ± 0.09	1.20 ± 0.05	1.29 ± 0.24	1.23 ± 0.19	1.04 ± 0.18	1.21 ± 0.21
	Ct. Th.	mm	0.14 ± 0.02	0.14 ± 0.01	0.17 ± 0.01	0.17 ± 0.02	0.77 ± 0.09	0.84 ± 0.13
	Imin	$\times 10^{-2}\ mm^4$	0.85 ± 0.08	.89 ± 0.03	1.33 ± 0.28	1.22 ± 0.38	1.18 ± 0.17	1.63 ± 0.55
	Ma.D.	pixel	154.01 ± 8.90	159.42 ± 2.55	152.30 ± 4.67	155.68 ± 4.84	166.26 ± 4.75	167.27 ± 2.68
n			5	5	5	5	4	6

BV/TV, bone volume versus tissue volume; Tb.N., trabecular number; Tb.Th., trabecular thickness; Tb. Sp., trabecular separation; T. Ar., tissue area; B.Ar., bone area; M.Ar., marrow area; Ct.Th., cortical thickness; Imin, minimum second moment of area; Ma.D., material density.

Values are means ± SD.

* $p<0.05$ versus WT mice by Student's t-Test.

Table 3

DMP1-*SOST* transgenic mice exhibit no changes in volume or geometry of ulna cortical bone or length of long bones

bone	parameters	unit	female (16-week-old)	
			WT	TG
ulna midshaft (cortical)	T.Ar.	mm^2	0.33 ± 0.02	0.31 ± 0.02
	B.Ar.	mm^2	0.27 ± 0.01	0.277 ± 0.005
	M.Ar.	mm^2	0.05 ± 0.01	0.05 ± 0.02
	Ct. Th.	mm	0.16 ± 0.01	0.16 ± 0.01
	Imin	$\times 10^{-2}$ mm^4	0.44 ± 0.04	0.38 ± 0.06
	Ma.D.	pixel	203.72 ± 5.82	210.37 ± 2.16
n			8	3

bone	parameters	unit	female (16-week-old)		male (16-week-old)	
			WT	TG	WT	TG
femur	length	mm	15.31 ± 0.50	15.14 ± 0.16	15.52 ± 0.33	15.10 ± 0.45
tibia	length	mm	17.74 ± 0.73	17.96 ± 0.29	18.08 ± 0.19	17.93 ± 0.29
n			6	5	5	5

T. Ar., tissue area; B.Ar., bone area; M.Ar., marrow area; Ct.Th., cortical thickness; Imin, minimum second moment of area; Ma.D., material density.

Values are means ± SD.